Dynamic Tracking of Non-Stationarity in Human ECoG Activity

Yuxiao Yang[1], *Student Member*, *IEEE*, Edward F. Chang[2], and Maryam M. Shanechi[1], *Member*, *IEEE*

***Abstract*— Modeling brain network dynamics is essential in understanding neural mechanisms and developing neurotechnologies such as closed-loop stimulation therapies for a wide range of neurological disorders. Brain network activity could have non-stationary and time-variant dynamics, especially when the subject's brain is monitored for a long period, e.g., using the electrocorticogram (ECoG). This non-stationarity makes the modeling of dynamics challenging. In our prior work, we developed a framework to identify time-invariant linear state-space models (SSMs) to describe both stationary spontaneous neural population dynamics and input-output (IO) neural dynamics in response to electrical stimulation. Here, we develop an adaptive identification algorithm that estimates time-variant SSMs to track possible non-stationarity in brain network dynamics. We apply the adaptive algorithm to track high-density human ECoG dynamics in three subjects over a long time-period. We find that the adaptive identification algorithm can estimate time-variant SSMs that significantly outperform time-invariant SSMs in all subjects. Our results demonstrate that non-stationary dynamics exist in high-dimensional human ECoG signals over long time-periods, and that the proposed adaptive SSM identification algorithm can successfully track these non-stationarities. These results have important implications for more accurate estimation of neural biomarkers for different brain states and for adaptive closed-loop stimulation therapy across a wide range of neurological disorders.**

I. INTRODUCTION

Identification and tracking of brain network dynamics is important both for understanding neural mechanisms and for developing various neurotechnologies. For example, such tracking is essential in uncovering biomarkers for neurological disorders such as depression [1] or developing adaptive closed-loop stimulation therapies, or brain-machine-interfaces (BMIs), to treat various neurological disorders [2], [3]. We have recently developed an identification framework to estimate time-invariant linear state-space models (SSMs) to describe spontaneous neural population dynamics [1], and input-output (IO) neural dynamics in response to electrical stimulation [2], [3]. We have shown that the SSM identification framework leads to time-invariant models that can successfully predict human electrocorticogram (ECoG) dynamics [1] and can help develop closed-loop stimulation therapies [3].

However, brain network dynamics could be non-stationary and time-variant in some cases, especially over long periods of days or weeks. Indeed various neurotechnologies, such as closed-loop brain stimulation systems, need to operate over these long periods. Hence the prediction power of a time-invariant SSM estimated with an offline batch of data can degrade over time. Developing adaptive models that can track non-stationarities could improve the prediction of brain network dynamics compared with time-invariant models, and in turn improve neural biomarker discovery and model-based closed-loop electrical stimulation systems.

Adaptive state-space identification methods have significantly improved the performance of spike-based closed-loop motor BMIs [4], [5] and electroencephalogram (EEG)-based closed-loop systems for anesthetic delivery [6]. In addition to spikes and EEG, ECoG provides a new recording modality that has a higher signal-to-noise ratio compared to EEG and could improve longevity compared to spikes. As such, ECoG holds great promise as the feedback signal to estimate the brain state. It is therefore important to examine the non-stationary nature of human ECoG network activity and to develop adaptive SSM identification algorithms to track its non-stationary dynamics online.

In this work, we first develop an adaptive subspace identification algorithm to estimate time-variant SSMs online. We introduce a forgetting factor and compute time-variant output covariances to deal with non-stationarity over time. We use recursive QR-decomposition [7] to enable online implementation of the algorithm. We then examine the non-stationary nature of high-density ECoG data (around 105 channels) recorded from three epilepsy patients by comparing the prediction of the time-variant SSM with a time-invariant SSM estimated with traditional non-adaptive subspace identification algorithms such as N4SID [8]. Spontaneous ECoG signals are continuously recorded over on average 5 days. We find that the proposed adaptive identification algorithm results in time-variant models that can predict the ECoG network dynamics better than the non-adaptive models in all three subjects. Our results show that non-stationary dynamics exist in high-dimensional human ECoG signals, and that the proposed adaptive identification algorithm can successfully track the non-stationary dynamics and improve the ECoG prediction power.

II. METHODS

A. Adaptive identification of state-space model

Under the assumption that brain network dynamics are stationary, our prior work [1], [2] has proposed time-invariant linear SSMs to predict ECoG dynamics. To model spontaneous human ECoG dynamics, we write this time-invariant linear SSM as

$$\begin{cases} \mathbf{x}_{t+1} &= \mathbf{A}\mathbf{x}_t + \mathbf{w}_t \\ \mathbf{y}_t &= \mathbf{C}\mathbf{x}_t + \mathbf{v}_t \end{cases} \quad (1)$$

[1]Yuxiao Yang and Maryam M. Shanechi are with the Department of Electrical Engineering, University of Southern California, Los Angeles, CA, 90089, USA shanechi at usc.edu.

[2]Edward F. Chang is with the Department of Neurological Surgery, University of California, San Francisco, San Francisco, CA, 94143.

978-1-5090-2809-2/17/$31.00 ©2017 IEEE

where $\mathbf{y}_t \in \mathbf{R}^{n_y}$ is the observed neural features, which we select as ECoG log-powers (Section II.B), $\mathbf{x}_t \in \mathbf{R}^{n_x}$ is a hidden state and $\mathbf{w}_t$ and $\mathbf{v}_t$ summarize modeling errors and unmeasured disturbances/inputs, and are modeled as white Gaussian noises with zero mean and covariance $\mathbb{E}\left[\begin{pmatrix}\mathbf{w}_i\\ \mathbf{v}_j\end{pmatrix}(\mathbf{w}_i^{'}\ \mathbf{v}_j^{'})\right] = \begin{pmatrix}\mathbf{Q} & \mathbf{S}\\ \mathbf{S}^{'} & \mathbf{P}\end{pmatrix}\delta_{ij}$ with $\delta_{ij} = 1$ if $i = j$ and 0 otherwise. Here $\cdot^{'}$ represents the transpose of a vector or a matrix. We can use subspace identification algorithms such as N4SID [8] to identify the time-invariant model parameters, including the model order n_x, system matrices $\mathbf{A} \in \mathbb{R}^{n_x \times n_x}$, $\mathbf{C} \in \mathbb{R}^{n_y \times n_x}$, and noise covariance matrices $\mathbf{Q} \in \mathbb{R}^{n_x \times n_x}$, $\mathbf{P} \in \mathbb{R}^{n_y \times n_y}$ and $\mathbf{S} \in \mathbb{R}^{n_x \times n_y}$.

The dynamics of long-term human ECoG recordings could be non-stationary, violating the assumption for the time-invariant model. Our goal is to develop an adaptive SSM identification framework to track the non-stationary dynamics. We thus build a time-variant linear SSM as follows

$$\begin{cases} \mathbf{x}_{t+1} &= \mathbf{A}_t\mathbf{x}_t + \mathbf{w}_t \\ \mathbf{y}_t &= \mathbf{C}_t\mathbf{x}_t + \mathbf{v}_t \end{cases} \quad (2)$$

Here, the system matrices $\mathbf{A}_t$, $\mathbf{C}_t$, and noise covariance matrices $\mathbf{Q}_t$, $\mathbf{R}_t$ and $\mathbf{S}_t$ are modeled to be time-variant. Tracking non-stationary dynamics is then equivalent to tracking these time-variant model parameters. To estimate these online, we develop an adaptive identification algorithm. For compactness of exposition, we omit the details of the algorithm and only briefly introduce some key components.

The core of traditional subspace algorithms such as N4SID consists of two step. 1) Compute the time-invariant output covariance matrices $\mathbf{\Lambda}_\tau = \mathbb{E}[\mathbf{y}_{t+\tau}\mathbf{y}_t^{'}] \propto \sum_{k=1}^{T}\mathbf{y}_{k+\tau}\mathbf{y}_k^{'}$, with T denoting the total time of recordings. 2) Estimate $\mathbf{A}$, $\mathbf{C}$, $\mathbf{Q}$, $\mathbf{P}$ and $\mathbf{S}$ from those output covariance matrices via subspace estimation techniques such as singular-value-decomposition [8]. To implement the algorithms in a robust and efficient way, QR-decomposition of a particular matrix formed by the outputs has been used [8]. From the upper triangular matrix R in this QR-decomposition, $\mathbf{A}$, $\mathbf{C}$, $\mathbf{Q}$, $\mathbf{P}$ and $\mathbf{S}$ can be efficiently calculated [8].

Here we develop a modified subspace learning algorithm to estimate time-variant SSMs online. The key idea is that, in contrast with traditional subspace algorithms, we estimate time-variant output covariance matrices as

$$\mathbf{\Lambda}_\tau(t) = \mathbb{E}[\mathbf{y}_{t+\tau}\mathbf{y}_t^{'}] \propto \sum_{k=1}^{t}\beta^{t-k}\mathbf{y}_{k+\tau}\mathbf{y}_k^{'} \quad (3)$$

where t is the current time and $\beta \in (0,1)$ is a user-defined constant forgetting factor. Thus, we update the estimate of output covariance matrices at every time step, where we put more weight on the recent data than past data.

Since we calculate new output covariance matrices at every time step, the QR-decomposition also needs to be recalculated at every time step. To enable online operation of the QR-decomposition, we use a recursive algorithm to update the R matrix in the QR-decompositions. Based on (3), after straightforward algebraic manipulations, the R matrix of the current time step, i.e., $\mathbf{R}_t$, can be calculated as

$$\mathbf{R}_t = \sqrt{\beta}\mathbf{G}_1\mathbf{R}_{t-1} + \mathbf{G}_2\tilde{\mathbf{y}}_t \quad (4)$$

where $\mathbf{R}_{t-1}$ is the R matrix of the previous time step, $\tilde{\mathbf{y}}_t = [\mathbf{y}_{t-d+2}^{'}, \mathbf{y}_{t-d+1}^{'}, ..., \mathbf{y}_t{}']$ is the current data vector, with d a user-defined delay factor, and $\mathbf{G}_1$, $\mathbf{G}_2$ are Givens rotation matrices calculated from $\mathbf{R}_{t-1}$ and $\tilde{\mathbf{y}}_t$ [7]. As the last step, we extract $\mathbf{A}_t$, $\mathbf{C}_t$, $\mathbf{Q}_t$, $\mathbf{P}_t$ and $\mathbf{S}_t$ from $\mathbf{R}_t$ following the procedures of standard subspace algorithms [8].

Together, these steps provide an adaptive identification algorithm to track ECoG non-stationarity over time.

B. ECoG data acquisition and processing

We collect high-density ECoG from three human epilepsy patients (S1 - S3) for on average five days (S1: 126 hours; S2: 111 hours; S3: 123 hours). We record from on average 105 (S1: 128; S2: 114; S3: 75) ECoG electrodes covering various brain regions at a sampling rate of 1kHz.

We use log-power features as the neural observations $\mathbf{y}_t$ (Fig. 1(a)). To obtain the log-power features, we first use common average referencing to remove common noises. Next, we use 10 second rectangular windows to divide the ECoG across time. For each window, we use multi-taper method [9] to estimate the power spectral density (PSD) of the windowed ECoG. We then calculate the log-powers of four frequency bands, [1 7]Hz, [8 12]Hz, [13 30]Hz, and [31 50]Hz. Consequently, we obtain a high-dimensional log-power time series, with an average dimension of 420 across subjects . To have a consistent number of total features across subjects, we randomly select 300 features as $\mathbf{y}_t$ (since S3 has the minimum total number of features, which is 300). Therefore, for each subject, $\mathbf{y}_t$ has a dimension of $n_y = 300$. Finally, for each component of $\mathbf{y}_t$, we remove the mean from the time-series to have zero mean outputs.

C. Training and testing of state-space model

For each subject, we divide $\mathbf{y}_t$ into training and testing datasets (Fig. 1(b)). Using the same training dataset, we estimate two SSMs by the adaptive and non-adaptive identification algorithms, referred to as $\mathrm{SSM}_{\mathrm{adpt}}$ and $\mathrm{SSM}_{\mathrm{non-adpt}}$, respectively. For the adaptive identification algorithm, we adaptively estimate the SSM till the end of the training dataset and then fix it as $\mathrm{SSM}_{\mathrm{adpt}}$ (Fig. 1(b)). For the non-adaptive identification algorithm, we train a single model $\mathrm{SSM}_{\mathrm{non-adpt}}$ using the entire batch of training data. We compare the prediction power of $\mathrm{SSM}_{\mathrm{adpt}}$ and $\mathrm{SSM}_{\mathrm{non-adpt}}$ on a subsequent testing dataset (Fig. 1(b)). Note that we don't further adapt the $\mathrm{SSM}_{\mathrm{adpt}}$ in the testing dataset. This means that both $\mathrm{SSM}_{\mathrm{adpt}}$ and $\mathrm{SSM}_{\mathrm{non-adpt}}$ are trained using the exact same data. By comparing the prediction power of the two models, we show that ECoG dynamics could be non-stationary and that the $\mathrm{SSM}_{\mathrm{adpt}}$ can better track ECoG dynamics in the testing dataset compared with $\mathrm{SSM}_{\mathrm{non-adpt}}$.

To make a comprehensive comparison between $\mathrm{SSM}_{\mathrm{adpt}}$ and $\mathrm{SSM}_{\mathrm{non-adpt}}$, we need to 1) use the same model order n_x for both models and 2) compare the models on multiple testing datasets. To estimate n_x, we use data from the first

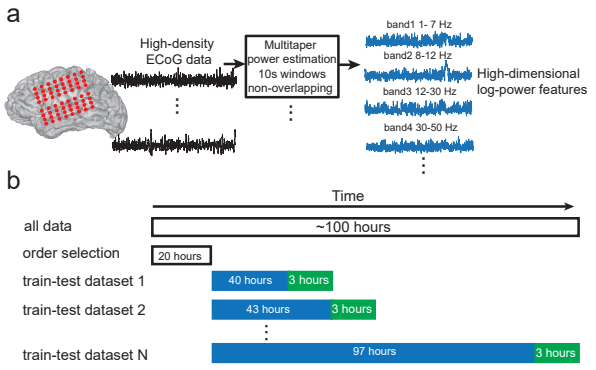

Fig. 1. Data processing procedure. (a) Calculation of ECoG log-power features. (b) Procedure of state-space model training and testing.

20 hours to estimate n_x by non-adaptive subspace algorithms and Akaike information criterion (AIC) [2]. We then fix n_x for both the adaptive and non-adaptive identification algorithm for subsequent SSM training (Fig. 1(b)).

To compare $\mathrm{SSM}_{\mathrm{adpt}}$ and $\mathrm{SSM}_{\mathrm{non-adpt}}$ on multiple testing datasets, we form "train-test" datasets as described below. We start form a 40-hour training and 3-hour testing "train-test" dataset (Fig. 1(b)). We train $\mathrm{SSM}_{\mathrm{adpt}}$ and $\mathrm{SSM}_{\mathrm{non-adpt}}$ on the 40-hour training dataset using algorithms introduced in Section II.A. Here we set $\beta = 0.9999$ and $d = 10$ in the adaptive identification algorithm for all subjects. We then compute the prediction power of $\mathrm{SSM}_{\mathrm{adpt}}$ and $\mathrm{SSM}_{\mathrm{non-adpt}}$ on the 3-hour testing dataset (section II.D). After this first "train-test" dataset, we successively enlarge the training dataset to form multiple "train-test" datasets. The last "train-test" dataset will cover all the data until the end of the ECoG log-power time series (Fig. 1(b)). For each "train-test" dataset, we repeat the model identification and performance assessment procedure. Finally, for every subject, we compare the prediction power of $\mathrm{SSM}_{\mathrm{adpt}}$ and $\mathrm{SSM}_{\mathrm{non-adpt}}$ on multiple testing sets (number of testing sets $N_{\mathrm{test}} = 22, 17, 21$ for the 3 subjects).

D. Performance measures on testing datasets

To compare the prediction power of $\mathrm{SSM}_{\mathrm{adpt}}$ and $\mathrm{SSM}_{\mathrm{non-adpt}}$ quantitatively, we caculate one-step-ahead prediction error [10] on testing datasets. For a given SSM with estimated parameters $\hat{\mathbf{A}}$, $\hat{\mathbf{C}}$, $\hat{\mathbf{Q}}$, $\hat{\mathbf{P}}$ and $\hat{\mathbf{S}}$, the one-step-ahead prediction of $\mathbf{y}_{t+1}$ provides an estimate of the neural features at time $t+1$ given their observations up to time t. This prediction is given by the following Kalman predictor [10]

$$\begin{cases} \hat{\mathbf{x}}_{t+1|t} &= \hat{\mathbf{A}}\hat{\mathbf{x}}_{t|t-1} + \hat{\mathbf{K}}(\mathbf{y}_t - \hat{\mathbf{C}}\hat{\mathbf{x}}_{t|t-1}) \\ \hat{\mathbf{y}}_{t+1|t} &= \hat{\mathbf{C}}\hat{\mathbf{x}}_{t+1|t} \end{cases} \tag{5}$$

with $\hat{\mathbf{K}} = (\hat{\mathbf{A}}\mathbf{X}\hat{\mathbf{C}}' + \hat{\mathbf{S}})(\hat{\mathbf{C}}\mathbf{X}\hat{\mathbf{C}}' + \hat{\mathbf{P}})^{-1}$, and matrix $\mathbf{X}$ obtained from the Ricatti equation $\mathbf{X} = \hat{\mathbf{A}}\mathbf{X}\hat{\mathbf{A}}' + \hat{\mathbf{Q}} - (\hat{\mathbf{A}}\mathbf{X}\hat{\mathbf{C}}' + \hat{\mathbf{S}})(\hat{\mathbf{C}}\mathbf{X}\hat{\mathbf{C}}' + \hat{\mathbf{P}})^{-1}(\hat{\mathbf{C}}\mathbf{X}\hat{\mathbf{A}}' + \hat{\mathbf{S}}')$. We initialize $\hat{\mathbf{x}}_{1|0} = 0$.

We define the relative prediction error (RPE) as

$$\mathrm{RPE} = \frac{1}{n_y}\sum_{i=1}^{n_y}\sqrt{\frac{\sum_{t=1}^{T_{\mathrm{test}}}(\hat{y}^{(i)}_{t|t-1} - y^{(i)}_t)^2}{\sum_{t=1}^{T}(y^{(i)}_t)^2}} \tag{6}$$

where T_{test} is the total number of time samples in a test dataset. We define $\mathrm{RPE}_{\mathrm{adpt}}$ and $\mathrm{RPE}_{\mathrm{non-adpt}}$ as the RPE of $\mathrm{SSM}_{\mathrm{adpt}}$ and $\mathrm{SSM}_{\mathrm{non-adpt}}$. For a particular SSM, we define the model to have significant prediction power if its RPE across testing datasets are significantly less than 1 ($p < 0.05$ in a Wilcoxon signed-rank test). This is because mean prediction, i.e., predicting the feature value simply as its mean (0 in our case) corresponds to RPE $= 1$ and provides no real prediction power.

Next, to better demonstrate the results, we introduce a baseline RPE using prediction errors on *training* datasets. We define $\mathrm{RPE}_{\mathrm{baseline}}$ as the minimum one of the RPEs of $\mathrm{SSM}_{\mathrm{adpt}}$ and $\mathrm{SSM}_{\mathrm{non-adpt}}$ on the training dataset. It's clear that $\mathrm{RPE}_{\mathrm{baseline}}$ is a lower bound of $\mathrm{RPE}_{\mathrm{adpt}}$ and $\mathrm{RPE}_{\mathrm{non-adpt}}$, since the latter are prediction errors on the *testing* dataset whereas the former is over the *training* dataset [11]. We next define a normalized RPE (NRPE) as RPE on a testing dataset normalized to $\mathrm{RPE}_{\mathrm{baseline}}$

$$\mathrm{NRPE} = \frac{\mathrm{RPE} - \mathrm{RPE}_{\mathrm{baseline}}}{\mathrm{RPE}_{\mathrm{baseline}}} \tag{7}$$

Finally, we summarize the improvement from $\mathrm{NRPE}_{\mathrm{non-adpt}}$ to $\mathrm{NRPE}_{\mathrm{adpt}}$ across testing datasets by the following error reduction percentage (ERP)

$$\mathrm{ERP} = \frac{\mathbb{E}[\mathrm{NRPE}_{\mathrm{non-adpt}}] - \mathbb{E}[\mathrm{NRPE}_{\mathrm{adpt}}]}{\mathbb{E}[\mathrm{NRPE}_{\mathrm{non-adpt}}]} \times 100\% \tag{8}$$

III. RESULTS

Next, we will show results from an example subject (S2, Fig. 2) followed by the overall results across subjects (Fig. 3).

First, consistent with our prior work [1], we confirmed that both $\mathrm{SSM}_{\mathrm{adpt}}$ and $\mathrm{SSM}_{\mathrm{non-adpt}}$ could predict the high-dimensional ECoG features. For S2, compared with mean prediction, both models had significant prediction power using an AIC-selected model order n_x of 28. That is, $\mathrm{RPE}_{\mathrm{adpt}}$ and $\mathrm{RPE}_{\mathrm{non-adpt}}$ were significantly below 1 across 17 testing datasets (Fig. 2(a) and (b), $p < 0.0005$). Note that all statistical tests are Wilcoxon signed-rank test in this section. The same results held across all 3 subjects ($p < 0.0005$).

Second, by examining some example predictions of $\mathrm{SSM}_{\mathrm{non-adpt}}$, we found that ECoG data could exhibit non-stationary dynamics. For example, in S2, we see that the trained $\mathrm{SSM}_{\mathrm{non-adpt}}$ can have large bias in predicting the true power features in the testing dataset (Fig. 2(c)). We hypothesize that this bias came from data non-stationarity since the training datasets spanned a long time-period (at least 40 hours). Hence the dynamics at the end of the training dataset could be different from the dynamics at the beginning of the training dataset. In this case, the average time-invariant model $\mathrm{SSM}_{\mathrm{non-adpt}}$ cannot adapt to the time-variations and thus has large prediction errors on the testing datasets ($\mathrm{RPE}_{\mathrm{adpt}} > 1$ in these two particular features). To confirm this hypothesis, we next examined the predictions of the time-variant model $\mathrm{SSM}_{\mathrm{adpt}}$ and found that $\mathrm{SSM}_{\mathrm{adpt}}$ can largely reduce the bias (Fig. 2(c)). This shows that non-stationarities indeed exist in human ECoG data.

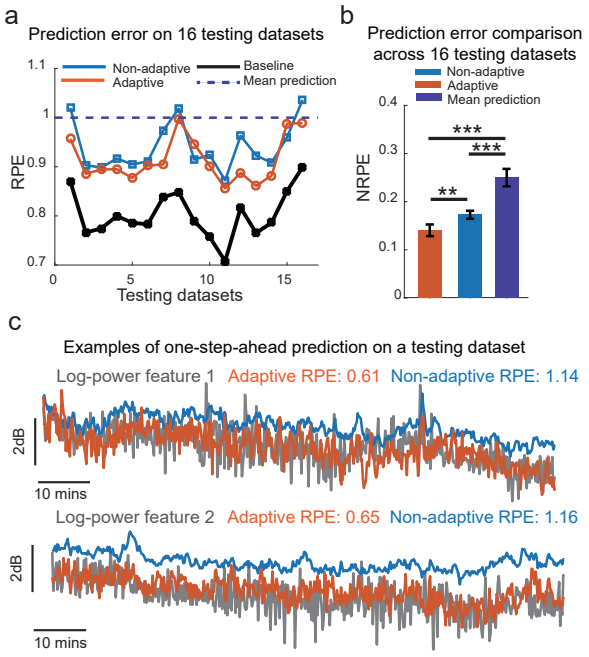

Fig. 2. Adaptive and non-adaptive tracking of ECoG dynamics in one subject. (a) Prediction errors on testing datasets. (b) Normalized relative prediction errors. Bars represent mean and whiskers represent standard error of the mean. * $p < 0.05$, ** $p < 0.005$, *** $p < 0.0005$. (c) Examples of prediction of output log-power features.

Third, by comparing the prediction powers (section II.D) of $\mathrm{SSM}_{\mathrm{adpt}}$ and $\mathrm{SSM}_{\mathrm{non-adpt}}$, we find that the proposed adaptive algorithm can successfully account for the non-stationarity. For example, in S2, $(\mathrm{N})\mathrm{RPE}_{\mathrm{adpt}}$ was significantly less than $(\mathrm{N})\mathrm{RPE}_{\mathrm{non-adpt}}$ across 16 testing datasets (Fig. 2(a) and (b), $p < 0.005$). This indicates that the time-variant model $\mathrm{SSM}_{\mathrm{adpt}}$ better captured the non-stationary dynamics than the time-invariant model $\mathrm{SSM}_{\mathrm{non-adpt}}$. The above results were consistent across subjects. For each subject, $\mathrm{SSM}_{\mathrm{adpt}}$ had significantly smaller NRPEs compared with $\mathrm{SSM}_{\mathrm{non-adpt}}$ across testing datasets (Fig. 3, $p < 0.005$). Across subjects, the error reduction percentage from $\mathrm{NRPE}_{\mathrm{non-adpt}}$ to $\mathrm{NRPE}_{\mathrm{adpt}}$ was on average 25% (Fig. 3). These results further confirm that non-stationary dynamics exist in human ECoG data. The results also demonstrate that the proposed adaptive algorithm can successfully estimate time-variant SSMs to track non-stationary dynamics, and can improve the prediction performance of time-invariant SSMs.

IV. CONCLUSIONS AND DISCUSSIONS

In this work, we develop an adaptive subspace identification algorithm to estimate time-variant state-space models that track non-stationary brain network dynamics. We apply this adaptive subspace identification algorithm to high-dimensional human ECoG data. We show that, compared to traditional non-adaptive identification algorithms, the proposed adaptive identification algorithm could better predict high-dimensional ECoG log-power time series in three human subjects. These results demonstrate that 1) human ECoG dynamics could be non-stationary over long time-periods and that 2) the presented adaptive SSM identification algorithm can track data non-stationarities and time-variations.

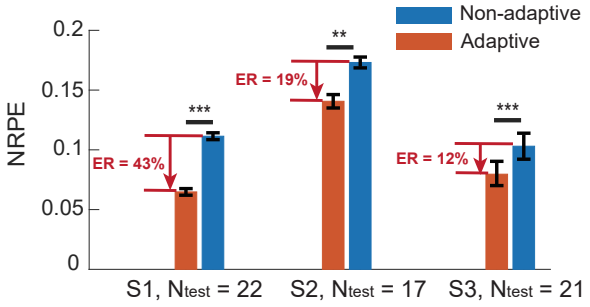

Fig. 3. Performance of $\mathrm{SSM}_{\mathrm{adpt}}$ and $\mathrm{SSM}_{\mathrm{non-adpt}}$ across three subjects.

Tracking non-stationary neural dynamics is essential for developing closed-loop stimulation systems that achieve better treatment of various neurological disorders. Adaptive model identification can lead to more precise estimation of neural biomarkers, and can facilitate the design of more effective feedback-controlled stimulation strategies. In addition, stimulation therapy might induce plasticity and changes in network dynamics. Stimulation induced plasticity is a special case of non-stationarity, and hence the adaptive algorithm has the potential to also track and account for plasticity effects. Our results thus have important implications for more accurate estimation of neural biomarkers and for better closed-loop stimulation therapies for a wide range of neurological disorders.

ACKNOWLEDGMENT

Support for this work was provided through DARPA/ARO. Contract #W911NF-14-2-0043.

REFERENCES

[1] A. T. Connolly, Y. Yang, E. F. Chang, and M. M. Shanechi, "Modeling brain network dynamics underlying mood disorders," in *Society for Neuroscience (SFN) Abstract, Chicago, IL, 2015*.

[2] Y. Yang and M. M. Shanechi, "A framework for identification of brain network dynamics using a novel binary noise modulated electrical stimulation pattern," in *Proc. IEEE Engineering in Medicine and Biology Society Conference (EMBC)*. 2015, pp. 2087–2090.

[3] Y. Yang and M. M. Shanechi, "Generalized binary noise stimulation enables time-efficient identification of input-output brain network dynamics," in *Proc. IEEE Engineering in Medicine and Biology Society Conference (EMBC)*. 2016, pp. 1766–1769.

[4] M. M. Shanechi, A. L. Orsborn, and J. M. Carmena, "Robust brain-machine interface design using optimal feedback control modeling and adaptive point process filtering," *PLoS Comput Biol*, vol. 12, no. 4, p. e1004730, 2016.

[5] V. Gilja, P. Nuyujukian, C. A. Chestek, J. P. Cunningham, M. Y. Byron, J. M. Fan, M. M. Churchland, M. T. Kaufman, J. C. Kao, S. I. Ryu, *et al.*, "A high-performance neural prosthesis enabled by control algorithm design," *Nat. Neurosci.*, vol. 15, no. 12, pp. 1752–1757, 2012.

[6] Y. Yang and M. M. Shanechi, "An adaptive and generalizable closed-loop system for control of medically induced coma and other states of anesthesia," *J. Neural Eng.*, vol. 13, no. 6, p. 066019, 2016.

[7] P. Strobach and D. Goryn, "A computation of the sliding window recursive qr decomposition," in *IEEE International Conference on Acoustics, Speech, and Signal Processing*, 1993, vol. 4. pp. 29–32.

[8] P. Van Overschee and B. L. De Moor, *Subspace identification for linear systems: theory, implementation, applications*. Kluwer academic publishers Dordrecht, 1996, vol. 3.

[9] D. J. Thomson, "Spectrum estimation and harmonic analysis," *Proceedings of the IEEE*, vol. 70, no. 9, pp. 1055–1096, 1982.

[10] L. Ljung, *System identification*. Wiley Online Library, 1999.

[11] J. Friedman, T. Hastie, and R. Tibshirani, *The elements of statistical learning*. Springer series in statistics Springer, Berlin, 2001, vol. 1.